

# Benzene Dimer: A Good Model for $\pi$ - $\pi$ Interactions in Proteins? A Comparison between the Benzene and the Toluene Dimers in the Gas Phase and in an Aqueous Solution

Christophe Chipot,<sup>\*,†,‡</sup> Richard Jaffe,<sup>§</sup> Bernard Maigret,<sup>⊥</sup> David A. Pearlman,<sup>||</sup> and Peter A. Kollman<sup>\*,†</sup>

Contribution from the Department of Pharmaceutical Chemistry, University of California, San Francisco, San Francisco, California 94143, Computational Chemistry Branch, NASA-Ames Research Center, Mail Stop 230-3, Moffett Field, California 94035-1000, Laboratoire de Chimie Théorique, Unité de Recherche Associée au CNRS No. 510, Université Henri Poincaré-Nancy I, BP. 239, 54506 Vandoeuvre-lès-Nancy Cedex, France, and Vertex Pharmaceuticals Incorporated, 40 Allston Street, Cambridge, Massachusetts 02139-4211

Received April 26, 1996. Revised Manuscript Received July 25, 1996<sup>Ⓞ</sup>

**Abstract:** We have investigated the relative orientational preference of two benzene and two toluene molecules in a *vacuum* and in water, by means of free energy calculations. The gas-phase simulations reveal that, whereas the T-shaped benzene dimer is 0.78 kcal/mol lower in free energy than its stacked homologue, the sandwich arrangement of the toluene dimer is preferred over the T-shaped structure by 0.18 kcal/mol. MP2/TZP ab initio binding energies, evaluated for both dimers, were found to be consistent with the molecular mechanical estimates, hence suggesting that the van der Waals and the electrostatic contributions to the macromolecular force field employed herein are well balanced. We further note that our results agree quite nicely with the experimental binding energies of Neusser and Krause, obtained from breakdown measurements. The tendency witnessed in the gas phase is magnified in an aqueous solution, with differences in free energy between the T-shaped and the sandwich arrangements of the benzene and the toluene dimers equal to -1.47 and 1.12 kcal/mol, respectively. The calculated association constants and osmotic second virial coefficients also correlate reasonably well with the experimental data of Tucker and Christian. The conflict between the orientational preferences of the benzene and the toluene dimers is suggestive that trends in " $\pi$ - $\pi$ " interactions in proteins should be rationalized by other factors than simple electrostatic/dispersion considerations. The analysis of Phe-Phe pairs in protein crystallographic structures sheds light on the influence of both sterical hindrances and ancillary interactions between the aromatic moieties and neighboring functional groups on the orientational preference of the phenyl rings.

## Introduction

For several years, it has been widely suggested that noncovalent interactions between aromatic moieties could play a key role in the conformational stability of a wide variety of chemical systems, with applications ranging from materials science to molecular biology. In particular, these interactions, prosaically called " $\pi$ - $\pi$ " interactions,<sup>1</sup> have been shown to influence the binding properties of nucleic acids,<sup>2</sup> the stability of proteins,<sup>3-9</sup> and the binding affinities in host-guest chemistry.<sup>10-13</sup> Yet,

despite having been the subject of intensive studies over the past decade, the nature of  $\pi$ - $\pi$  interactions is not unequivocally understood.

Whereas, in the case of nucleotide base interactions, face-to-face stacked arrangements of aromatic rings are commonly observed<sup>14,15</sup>—albeit nucleic bases never totally overlap, and are generally twisted away from a "true" stacked motif<sup>2</sup>—the pioneering analysis of protein structures by Burley and Petsko,<sup>4</sup> followed by that of Hunter *et al.*,<sup>8</sup> tend to indicate that T-shaped conformations are preferred in proteins. The latter conjecture agrees with several experimental studies,<sup>16-18</sup> as well as the earlier ab initio calculations of Pawliszyn *et al.*,<sup>19</sup> carried out on the prototypical benzene homodimer, which revealed the

<sup>†</sup> University of California.

<sup>‡</sup> On leave from: Laboratoire de Chimie Théorique, Unité de Recherche Associée au CNRS No. 510, Université Henri Poincaré-Nancy I, BP. 239, 54506 Vandoeuvre-lès-Nancy Cedex, France. Current address: Planetary Biology Branch, NASA-Ames Research Center, Mail Stop 239-4, Moffett Field, California 94035-1000.

<sup>§</sup> NASA-Ames Research Center.

<sup>⊥</sup> Université Henri Poincaré-Nancy I.

<sup>||</sup> Vertex Pharmaceuticals Incorporated.

<sup>Ⓞ</sup> Abstract published in *Advance ACS Abstracts*, November 1, 1996.

(1) Hunter, C. A.; Sanders, J. K. M. *J. Am. Chem. Soc.* **1990**, *112*, 5525.

(2) Saenger, W. *Principles of Nucleic Acid Structure*; Springer-Verlag: New York, 1984.

(3) Warne, P. K.; Morgan, R. S. *Biochemistry* **1978**, *118*, 273.

(4) Burley, S. K.; Petsko, G. A. *Science* **1985**, *229*, 23.

(5) Singh, J.; Thornton, J. M. *FEBS Lett.* **1985**, *191*, 1.

(6) Blundell, T.; Singh, J.; Thornton, J.; Burley, S. K.; Petsko, G. A. *Science* **1986**, *234*, 1005.

(7) Burley, S. K.; Petsko, G. A. *Adv. Protein Chem.* **1988**, *39*, 125.

(8) Hunter, C. A.; Singh, J.; Thornton, J. M. *J. Mol. Biol.* **1991**, *218*, 837.

(9) Serrano, L.; Bycroft, A. R. *J. Mol. Biol.* **1991**, *218*, 465.

(10) Lehn, J. M.; Schmidt, F.; Vigneron, J. P. *Tetrahedron Lett.* **1988**, *29*, 5255.

(11) Muehldorf, A. V.; Van Engen, D.; Warner, J. C.; Hamilton, A. D. *J. Am. Chem. Soc.* **1988**, *110*, 6561.

(12) Smithrud, D. B.; Diederich, F. *J. Am. Chem. Soc.* **1990**, *112*, 339.

(13) Ferguson, S. B.; Sanford, E. M.; Seward, E. M.; Diederich, F. *J. Am. Chem. Soc.* **1991**, *113*, 5410.

(14) Lowe, M. J.; Schellman, J. A. *J. Mol. Biol.* **1972**, *65*, 91.

(15) Ts'o, P. O. P. In *Basic Principles of Nucleic Acid Chemistry*; Ts'o, P., Ed.; Academic Press: New York, 1974; Vol. 1, Chapter 6.

(16) Janda, K. C.; Hemminger, J. C.; Winn, J. S.; Novick, S. E.; Harris, S. J.; Klemperer, W. *J. Chem. Phys.* **1975**, *63*, 1419.

(17) Steed, J. M.; Dixon, T. A.; Klemperer, W. *J. Chem. Phys.* **1979**, *70*, 4940.

(18) Börnsen, K. O.; Selzle, H. L.; Schlag, E. W. *J. Chem. Phys.* **1986**, *85*, 1726.

(19) Pawliszyn, J.; Szczeniński, M. M.; Scheiner, S. *J. Phys. Chem.* **1984**, *88*, 1726.

T-shaped motif to be more stable than the stacked one. Although the small basis set employed by these authors arguably calls into question the accuracy of their results, it was shown that dispersion forces play a non-negligible role in the stabilization of  $\pi$ - $\pi$  arrangements. Interestingly enough, it should be noted that T-shaped conformations are also frequently found in crystalline benzene, as has been underlined earlier by Cox *et al.*<sup>20</sup> The very recent experimental studies of Henson *et al.*<sup>21</sup> and of Arunan *et al.*<sup>22</sup> converged toward the same conclusion, indicating that the T-shaped motif is markedly more stable than the sandwich one—yet, a so-called “parallel-displaced” structure has been shown to be even lower in energy than the T-shaped dimer,<sup>18,23</sup> but, because it has a zero permanent dipole, it was not observed in the latter spectroscopy experiments. Both the configuration interaction calculation of Karlström *et al.*<sup>24</sup> and the studies of Hobza *et al.*<sup>25–28</sup> provide a rationalization to these observations, and demonstrate that the electrostatic interaction in the benzene dimer, which is dominated by the  $1/r^5$  quadrupole–quadrupole component, is attractive for the T-shaped arrangement and repulsive for the stacked one.

Conversely, London dispersion forces are expected to be more favorable for the face-to-face stacked dimer. In addition, when solvated, this conformation has a smaller area exposed toward the solvent than the point-to-face T-shaped motif.<sup>29</sup> This would suggest that, if embedded in an aqueous medium, hydrophobic effects would favor  $\pi$ -overlaps at the expense of perpendicular—or nearly perpendicular—arrangements of the aromatic rings.

That this is not completely true is reported by Jorgensen and Severance,<sup>30</sup> who investigated an orientationally averaged benzene homodimer in water. From their Monte Carlo (MC) potential of mean force (PMF) simulation, these authors found two distinct minima clearly suggesting that face-to-face stacked arrangements are generally disfavored. This work was subsequently corroborated by the classical molecular dynamics (MD) PMF simulations of Linse,<sup>29,31</sup> who showed on a related molecular system, but using a more sophisticated potential energy function,<sup>32</sup> that the T-shaped motif is thermodynamically preferred over the stacked one. Point-to-face and edge-to-face arrangements have been explained to be the result of interacting electric fields around the benzene rings,<sup>16,17</sup> but, is it really so? As noted by Jorgensen and Severance, the electrostatic contribution to the total energy appears to be relatively small when compared with that arising from London dispersion forces.<sup>30</sup> Not mentioning charge transfer or electron donor–acceptor effects—undoubtedly negligible in comparison with electrostatic interactions<sup>33,34</sup>—it would seem that dispersion is the driving

force of most  $\pi$ - $\pi$  interactions. As underlined by Hunter,<sup>35,36</sup> another important component responsible for additional stabilization of aromatic–aromatic complexes in polar solvent (*viz.* typically water) can be ascribed to solvophobic effects.

In the present contribution, we analyze quantitatively the magnitude of the noncovalent  $\pi$ - $\pi$  interactions between two benzene molecules and two toluene molecules, embedded in an aqueous solution, by means of molecular dynamics potential of mean force calculations. Toluene can be viewed as the modeled side chain of phenylalanine (Phe). Although incomplete and prototypical, this molecule constitutes a reasonably better reduced model of the Phe side chain than the simple benzene, which has been hitherto utilized as a paradigm to rationalize various analysis of protein X-ray structures. We will show that the different nature of the  $\pi$ - $\pi$  interactions characterizing the benzene and the toluene homodimers<sup>37</sup> leads to distinct orientational preferences. As a corollary, we will demonstrate that arguments based on either quantum mechanical (QM) or molecular mechanical (MM) calculations on the archetypical benzene dimer to account for trends in  $\pi$ - $\pi$  interactions within protein structures might be *non sequitur*, as such arguments do not necessarily hold for the toluene dimer. To support our assertions, we have evaluated the free energy profiles of the face-to-face stacked, the point-to-face T-shaped, and the orientationally averaged benzene and toluene dimers, in a *vacuum* and in an aqueous medium. In order to further validate our conclusions, we have carried out high-quality MP2/TZP *ab initio* QM calculations on those homodimers, and have confronted the latter with our gas-phase molecular mechanical results.

## Method—Computational Details

The goal of the present work is to compute the potentials of mean force (PMF) characterizing the approach of two benzene molecules and two toluene molecules as a function of an appropriately defined intermolecular distance. On the path along which the two solutes are brought together, the dimers will be considered in (i) a point-to-face T-shaped, (ii) a face-to-face stacked, and (iii) an orientationally averaged conformation. Thermodynamic integration<sup>38–41</sup> (TI) was utilized to evaluate the free energy change between two given points of the PMF curve. The classical Hamiltonian—or potential energy function—employed for the various molecular simulations described in this contribution is the one developed by Weiner *et al.*<sup>42,43</sup> Use was made of the standard mixing rules:  $r_{ij}^* = (r_i^* + r_j^*)/2$  and  $\epsilon_{ij} = (\epsilon_i \epsilon_j)^{1/2}$ . The effective dielectric constant,  $\epsilon$ , was set to 1.0.

We have shown that TI often leads to a better convergence of the free energy when the integrand is evaluated at a limited number of “ $\lambda$ ” points involving extensive sampling<sup>44,45</sup> (assuming a reasonably slowly varying  $\Delta G$  versus  $\lambda$  curve). For all the PMF simulations reported herein, no more than 100 points were employed to change the distance between centroids of the aromatic rings (see Figure 1). In the case of the benzene dimer, the intersolute distance was progressively decreased from 9.5 to 4.0 Å, for the T-shaped conformation, from 8.0 to 2.5 Å,

(20) Cox, E. G.; Cruickshank, D. W.; Smith, J. A. S. *Proc. R. Soc. London, Ser. A* **1958**, 247, 1.

(21) Henson, B. F.; Hartland, G. V.; Venturo, V. A.; Felker, P. M. *J. Chem. Phys.* **1992**, 97, 2189.

(22) Arunan, E.; Gutowsky, H. S. *J. Chem. Phys.* **1993**, 98, 4294.

(23) Law, K. S.; Schauer, M.; Bernstein, E. R. *J. Chem. Phys.* **1984**, 81, 4871.

(24) Karlström, G.; Linse, P.; Wallqvist, A.; Jönsson, B. *J. Am. Chem. Soc.* **1983**, 105, 3777.

(25) Hobza, P.; Selzle, H. L.; Schlag, E. W. *J. Chem. Phys.* **1990**, 93, 5893.

(26) Hobza, P.; Selzle, H. L.; Schlag, E. W. *J. Phys. Chem.* **1993**, 97, 3937.

(27) Hobza, P.; Selzle, H. L.; Schlag, E. W. *J. Am. Chem. Soc.* **1994**, 116, 3500.

(28) Hobza, P.; Selzle, H. L.; Schlag, E. W. *Chem. Rev.* **1994**, 94, 1767.

(29) Linse, P. *J. Am. Chem. Soc.* **1992**, 114, 4366.

(30) Jorgensen, W. L.; Severance, D. L. *J. Am. Chem. Soc.* **1990**, 112, 4768.

(31) Linse, P. *J. Am. Chem. Soc.* **1993**, 115, 8793.

(32) Linse, P. *J. Am. Chem. Soc.* **1990**, 112, 1744.

(33) Cozzi, F.; Cinquina, M.; Annuziata, R.; Dwyer, T.; Siegel, J. S. *J. Am. Chem. Soc.* **1992**, 114, 5729.

(34) Cozzi, F.; Cinquina, M.; Annuziata, R.; Siegel, J. S. *J. Am. Chem. Soc.* **1993**, 115, 5330.

(35) Hunter, C. A. *Angew. Chem., Int. Ed. Engl.* **1993**, 32, 1584.

(36) Hunter, C. A. *Chem. Soc. Rev.* **1994**, 23, 101.

(37) Neusser, H. J.; Krause, H. *Chem. Rev.* **1994**, 94, 1829.

(38) Mezei, M.; Beveridge, D. L. *Ann. N.Y. Acad. Sci.* **1986**, 482, 1.

(39) Beveridge, D. L.; DiCapua, F. M. *Annu. Rev. Biophys. Biophys. Chem.* **1989**, 18, 431.

(40) Mruzik, M. R.; Abraham, F. F.; Schreiber, D. E.; Pound, G. M. *J. Chem. Phys.* **1976**, 64, 481.

(41) Mezei, M.; Swaminathan, S.; Beveridge, D. L. *J. Am. Chem. Soc.* **1978**, 100, 3255.

(42) Weiner, S. J.; Kollman, P. A.; Case, D. A.; Singh, U. C.; Ghio, C.; Alagona, G.; Profeta, S., Jr.; Weiner, P. *J. Am. Chem. Soc.* **1984**, 106, 765.

(43) Weiner, S. J.; Kollman, P. A.; Nguyen, D. T.; Case, D. A. *J. Comput. Chem.* **1986**, 7, 230.

(44) Pearlman, D. A. *J. Chem. Phys.* **1993**, 98, 8946.

(45) Chipot, C.; Kollman, P. A.; Pearlman, D. A. *J. Comput. Chem.* **1996**, 17, 1112.

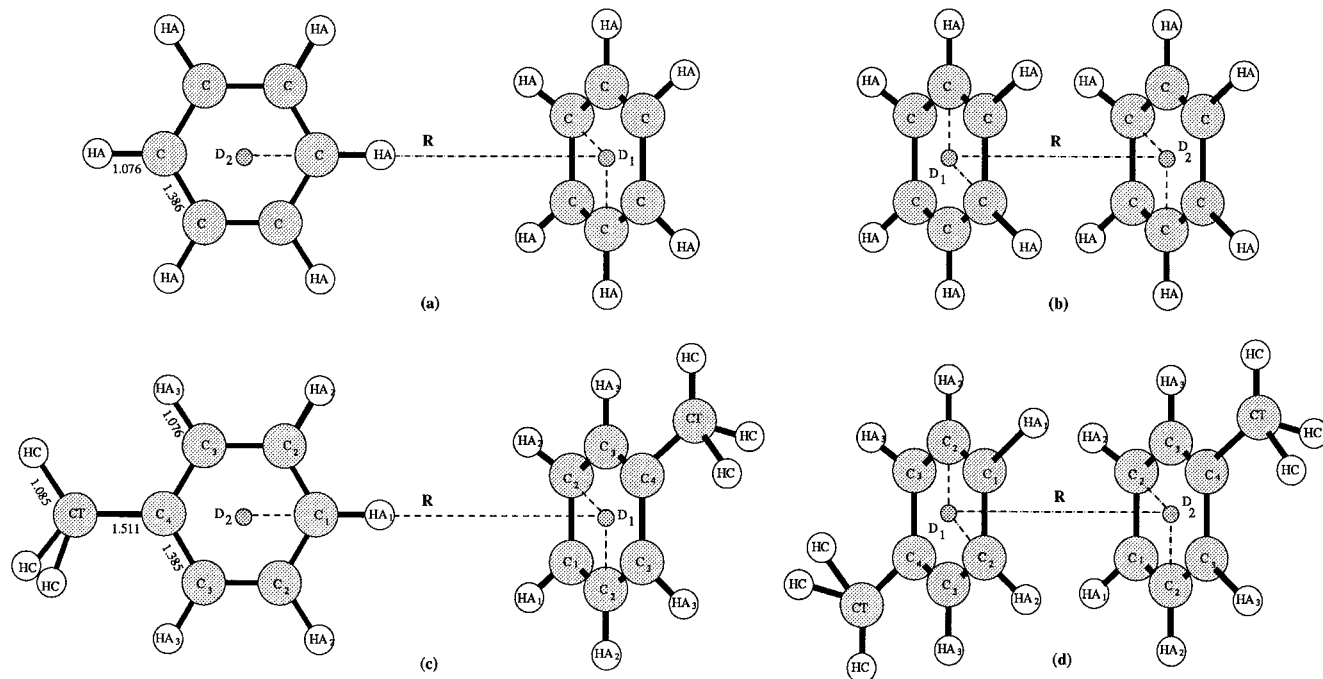


**Figure 1.** Geometrical parameters and atom types used for the MD simulations of the T-shaped and the stacked benzene (a and b) and toluene (c and d) dimers. All bond lengths in Å. Two pseudo-atoms “D<sub>i</sub>”, located at the center of the rings, are used to define the constrained distance “R” for the PMF calculations.

for the stacked conformation, and from 9.5 to 3.0 Å, for the orientationally averaged conformation. Conversely, in the case of the toluene dimer, the separation between the aromatic rings was diminished from 10.5 to 4.0 Å, for the T-shaped motif, from 8.0 to 2.5 Å, for the stacked motif, and from 10.5 to 3.0 Å, for the orientationally averaged conformation. At each “ $\lambda$ ” point, the intersolute distance was kept fixed using an appropriate holonomic constraint.<sup>46</sup> In order to maintain both the benzene and the toluene dimers in their T-shaped, or in their stacked, conformation, we have defined a series of additional angular constraints  $\{D_1, D_2, C_i\}$  set to the fixed value of 90.0°, maintaining the 6-fold  $C_6$  symmetry axis of the two aromatic rings perpendicular or colinear, respectively. We have opted for angular constraints rather than dihedral ones, so that phenyl rings may rotate freely about their 6-fold symmetry axis. The  $\lambda$  dependence of the constrained distance separating the noninteracting centroids of the benzene and the toluene rings is introduced in the TI formulation *via* the potential force (PF) method,<sup>44</sup> allowing a fast and accurate determination of  $\partial H^{\text{constr}}(\mathbf{r};\lambda)/\partial\lambda$ , the holonomic constraint contribution to the free energy.

All the PMF computations were carried out using the molecular simulation package GIBBS/AMBER 4.1<sup>47</sup> and the new Cornell *et al.*<sup>48</sup> van der Waals parameters, supplemented by potential derived net atomic charges<sup>49,50</sup> (see Table 1). The geometries of the solutes (see Figure 1) were optimized at the Hartree-Fock (HF) level of approximation, using the split-valence 6-31G\*\* basis set,<sup>51</sup> and the point charge distributions were determined from the corresponding wave functions. The standard AMBER force constants<sup>48</sup> were employed to evaluate the intramolecular interactions. Periodic boxes of 568, 498, and 568 TIP3P<sup>52</sup> water molecules were used to describe the solvent, in the case of the T-shaped, the stacked, and the unconstrained dimers of benzene,

(46) Tobias, D. J.; Brooks, C. L., III *J. Chem. Phys.* **1988**, *89*, 5115.

(47) Pearlman, D. A.; Case, D. A.; Caldwell, J. C.; Ross, W. S.; Cheatham, T. C.; Seibel, G.; Singh, U. C.; Weiner, P.; Kollman, P. A. *AMBER 4.1*; University of California, San Francisco (UCSF), San Francisco, 1994.

(48) Cornell, W. D.; Cieplak, P.; Bayly, C. I.; Gould, I. R.; Merz, K. M., Jr.; Ferguson, D. M.; Spellmeyer, D. C.; Fox, T.; Caldwell, J. C.; Kollman, P. A. *J. Am. Chem. Soc.* **1995**, *117*, 5179.

(49) Cox, S. R.; Williams, D. E. *J. Comput. Chem.* **1981**, *2*, 304.

(50) Chipot, C.; Angyán, J. G. *GRID Version 3.0: Point Multipoles Derived From Molecular Electrostatic Properties*; QCPE No. 655, 1994; Version 3.1 currently available.

(51) Hariharan, P. C.; Pople, J. A. *Chem. Phys. Lett.* **1972**, *16*, 217.

(52) Jorgensen, W. L.; Chandrasekhar, J.; Madura, J. D.; Impey, R. W.; Klein, M. L. *J. Chem. Phys.* **1983**, *79*, 926.

**Table 1.** Nonbonded Parameters Used in the Molecular Simulations

molecule <sup>a</sup>	atom type	charges (ecu)	Lennard-Jones parameters	
			$r_{ii}^*$ (Å)	$\epsilon_{ii}$ (kcal/mol)
benzene	C	-0.138	1.9080	0.0860
	HA	0.138	1.4590	0.0150
	D	0.000	0.0000	0.0000
toluene	C <sub>1</sub>	-0.189	1.9080	0.0860
	HA <sub>1</sub>	0.151	1.4590	0.0150
	C <sub>2</sub>	-0.128	1.9080	0.0860
	HA <sub>2</sub>	0.147	1.4590	0.0150
	C <sub>3</sub>	-0.279	1.9080	0.0860
	HA <sub>3</sub>	0.158	1.4590	0.0150
	C <sub>4</sub>	0.353	1.9080	0.0860
	CT	-0.574	1.9080	0.1094
	HC	0.154	1.4870	0.0157
TIP3P water <sup>52</sup>	OW	-0.834	1.7680	0.1520
	HW	0.417	0.0000	0.0000

<sup>a</sup> See Figure 1.

respectively. Similarly, boxes of 643, 525, and 643 TIP3P water molecules were built to solvate the T-shaped, the stacked, and the unconstrained dimers of toluene, respectively. We note in passing that, for benzene, the AMBER-Cornell *et al.* force field yielded a free energy of hydration<sup>45</sup> equal to  $-0.40 \pm 0.06$  kcal/mol, in good agreement with the experimental value of  $-0.767$  kcal/mol of Ben-Naim and Marcus.<sup>53</sup>

For each simulation, a hard cutoff of 9.0 Å was considered to truncate both the solute-solvent and the solvent-solvent interactions. All the free energy profiles were anchored to zero at an intermolecular distance of 8.0 Å for the stacked dimers, and 10.5 Å for the T-shaped and unconstrained ones. The time-step for integrating the MD trajectories was set to 1.0 fs, and the average temperature and pressure were maintained at 300 K and 1 atm, respectively, employing the Berendsen *et al.* weak coupling algorithm.<sup>54</sup> For the temperature, use was made of a separate coupling to an external heat bath for the solutes and for the solvent. Each bond length was constrained to its equilibrium value by means of the SHAKE<sup>55,56</sup> procedure. Finally, for each run, a 1 ns

(53) Ben-Naim, A.; Marcus, Y. *J. Chem. Phys.* **1984**, *81*, 2016.

(54) Berendsen, H. J. C.; Postma, J. P. M.; Van Gunsteren, W. F.; DiNola, A.; Haak, J. R. *J. Chem. Phys.* **1984**, *81*, 3684.

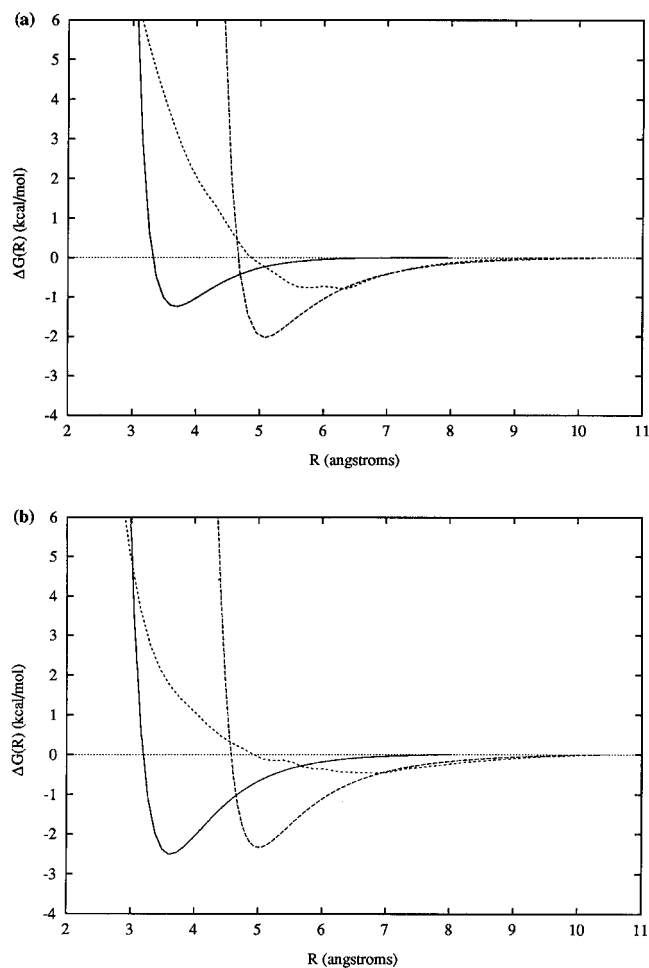


**Figure 2.** Free energy profiles of the stacked (solid line), the T-shaped (long-dashed line), and the unconstrained (short-dashed line) benzene (a) and toluene (b) dimers, in the gas phase.

classical molecular dynamics (MD) trajectory<sup>57</sup> was computed to generate the statistical ensembles<sup>58</sup> over which the quantity  $\partial H(\mathbf{r};\lambda)/\partial\lambda$  was averaged.

## Results—Discussion

**$\pi$ – $\pi$  Interactions in the Gas Phase.** The free energy profiles representing the mutual approach of the two benzene rings and the two toluene rings, in their point-to-face, face-to-face, and orientationally averaged conformations, in a *vacuum*, are shown in Figure 2. From the onset, the most striking difference between the two sets of curves lies in the hierarchy of the binding free energies characterizing the noncovalent interactions between these  $\pi$ -systems (see Table 2). In the case of benzene, the minimum corresponding to the T-shaped motif occurs at a distance separating the centroids of the two rings equal to 5.1 Å, with a free energy of  $-2.03$  kcal/mol. The minimum representative of the stacked complex, however, occurs at an intermolecular separation of 3.7 Å, with a binding

(55) Ryckaert, J.; Cicotti, G.; Berendsen, H. J. C. *J. Comput. Phys.* **1977**, *32*, 327.

(56) Van Gunsteren, W. F.; Berendsen, H. J. C. *Mol. Phys.* **1977**, *34*, 1311.

(57) In the case of the benzene dimer, use was made of 100 windows involving 2.5 ps of equilibration followed by 7.5 ps of data collection for the T-shaped motif ( $\delta R = 0.055$  Å), and 50 windows involving 5.0 ps of equilibration followed by 15.0 ps of data collection for both the stacked ( $\delta R = 0.110$  Å) and the orientationally-averaged ( $\delta R = 0.130$  Å) motifs. Identical protocols were employed for the three different motifs of the toluene dimer, at the exception of the T-shaped conformation, for which  $\delta R = 0.065$  Å.

(58) Karplus, M.; McCammon, J. A. *Annu. Rev. Biochem.* **1983**, *52*, 263.

**Table 2.** Estimated Relative Free Energies of the “Contact” and the “Solvent-Separated” Complexes of the Benzene and the Toluene Dimers, in *Vacuo* and in TIP3P Water

	“contact”		“solvent-separated”	
	$R_{D_1-D_2}$ (Å)	$\Delta G(R_{D_1-D_2})$ (kcal/mol)	$R_{D_1-D_2}$ (Å)	$\Delta G(R_{D_1-D_2})$ (kcal/mol)
benzene				
T-shaped	5.08 <sup>a</sup> 4.94 <sup>b</sup>	-2.03 <sup>a</sup> -1.94 <sup>b</sup>		
stacked	3.71 <sup>a</sup> 3.60 <sup>b</sup>	-1.25 <sup>a</sup> -0.47 <sup>b</sup>	7.96 <sup>b</sup>	-0.74 <sup>b</sup>
unconstrained	6.25 <sup>a</sup> 5.60 <sup>b</sup>	-0.78 <sup>a</sup> -0.36 <sup>b</sup>		
toluene				
T-shaped	5.00 <sup>a</sup> 4.95 <sup>b</sup>	-2.33 <sup>a</sup> -2.29 <sup>b</sup>	8.13 <sup>b</sup>	-0.85 <sup>b</sup>
stacked	3.60 <sup>a</sup> 3.49 <sup>b</sup>	-2.51 <sup>a</sup> -3.41 <sup>b</sup>	6.68 <sup>b</sup>	-0.80 <sup>b</sup>
unconstrained	6.66 <sup>a</sup> 5.38 <sup>b</sup>	-0.46 <sup>a</sup> -0.75 <sup>b</sup>		

<sup>a</sup> In *vacuo*. <sup>b</sup> In TIP3P water.<sup>52</sup>

free energy of  $-1.25$  kcal/mol, that is 0.78 kcal/mol weaker than that of the T-shaped dimer. Conversely, the T-shaped complex of the toluene dimer is characterized by a minimum occurring at an intermolecular distance of 5.0 Å, with a depth of  $-2.33$  kcal/mol, whereas the stacked motif arises at 3.6 Å, with a binding free energy of  $-2.51$  kcal/mol, that is 0.18 kcal/mol stronger than that of the T-shaped dimer.

Considering the reasonably similar chemical nature of benzene and toluene, one would expect their respective dimers to adopt similar conformational preferences. This may not be necessarily true: the repulsive quadrupole–quadrupole interactions occurring in the face-to-face motif of the benzene dimer dominates the attractive dispersion contribution arising from the stacked atoms. The observed favorableness of a sandwich structure in the case of toluene can be related to two cumulative effects, namely, (i) the small dipole borne by toluene gives rise to an attractive dipole–dipole interaction susceptible to counterbalance the repulsive quadrupole–quadrupole contribution, but, more significantly, (ii) the extra methyl group is responsible for an increase of the dispersion effects of approximately 40%.

Upon MM restrained energy minimization, during which the phenyl rings were artificially kept in either a point-to-face or a face-to-face motif, a similar trend was observed. The minimum corresponding to the stacked dimer of benzene occurred at 3.7 Å, with a binding energy of  $-1.30$  kcal/mol, whereas the minimum characterizing the T-shaped arrangement arose at an intermolecular distance of 5.1 Å, with a binding energy of  $-2.27$  kcal/mol. These results agree quite well with the binding energies of Jorgensen and Severance<sup>30</sup> ( $-1.70$  and  $-2.32$  kcal/mol for the stacked and the T-shaped dimers, respectively), as well as the most recent estimate of Nagy *et al.*<sup>59</sup> of  $-2.07$  kcal/mol for the sandwich arrangement. As expected, the stacked configuration of the toluene dimer, corresponding to an intermolecular distance of 3.5 Å, and a binding energy of  $-2.61$  kcal/mol, is energetically more favorable than the perpendicular arrangement, the energy minimum of which occurs at 5.1 Å, with a depth of  $-1.95$  kcal/mol.

In order to ascertain the accuracy of the above MM gas-phase calculations, we have endeavored to carry out a series of high-quality *ab initio* calculations at the second-order Møller–Plesset level of approximation. The 6-311G(2d,2p) and 6-31+G(2d,p)

(59) Nagy, J.; Smith, V. H., Jr.; Weaver, D. F. *J. Phys. Chem.* **1995**, *99*, 13868.

**Table 3.** Estimated Relative Binding Energies for the T-Shaped and the Stacked Conformations of the Benzene and the Toluene Dimers

“ $\pi$ - $\pi$ ” complex <sup>a</sup>	ab initio <sup>b</sup>		molecular mechanics	
	$R_{D_1-D_2}$ (Å)	$\Delta E^{MP2}$ (kcal/mol)	$R_{D_1-D_2}$ (Å)	$\Delta E^{AMBER}$ (kcal/mol)
benzene				
T-shaped	5.0	-2.84	5.1	-2.27
stacked	3.8	-2.13	3.7	-1.30
toluene				
T-shape	5.0	-2.72	5.1	-1.95
stacked	3.8	-3.43	3.5	-2.61

<sup>a</sup> See Figure 1. <sup>b</sup> BSSE corrected MP2/6-311G(2d,2p) and MP2/6-31G+(2d,p) ab initio calculations for the benzene and the toluene dimers, respectively.

basis sets were employed for the benzene and the toluene dimers, respectively. Jaffe and Smith have recently underlined that the inclusion of 2d orbitals is a *sine qua non* condition for a correct reproduction of dispersion effects.<sup>60,61</sup> In the first step of our calculations, the geometry of the monomers was optimized. During the subsequent optimizations of the structure of the various dimers, assumption was made that the geometry of the individual monomers was not affected significantly, and could, therefore, be frozen, while only the intermolecular distance would be modified. The basis set superposition error (BSSE) was estimated at each step. Whereas in the case of the benzene dimer, the point-to-face motif was found to be 0.71 kcal/mol lower in energy than the sandwich one, an opposite situation is observed for the toluene dimer (see Table 3). The stacked arrangement is 0.71 kcal/mol energetically more favorable than the T-shaped one. Put together, these data agree generally well with the above MM calculations, and clearly suggest that, indeed, the orientational preferences of the benzene and the toluene homodimers are different.

Neusser and Krause have recently reported experimental dissociation energies obtained by breakdown measurements, using a linear reflectron time-of-flight mass spectrometer (RETOF). The binding energy for the benzene dimer, which they mainly attribute to dispersion forces, is -1.6 kcal/mol. The agreement between this result and our molecular mechanical estimates is somewhat better for the stacked motif (-1.30 kcal/mol) than for the T-shaped one (-2.27 kcal/mol)—it should be pointed out, however, that the experimental data are representative of the lowest vibrational energy levels and correspond to  $-D_0$ , whereas our QM calculations provide an estimate of  $-D_e$ . In addition, compared to experiment, the quantum mechanically calculated energies are between 0.5 and 1.2 kcal/mol too attractive. A very similar trend can be witnessed in the data of Hobza *et al.*,<sup>27,28</sup> who employed a DZ+2P basis set. Inclusion of the zero-point energy (ZPE), which has been estimated coarsely to be *ca.* 0.5 kcal/mol, leads to an experimental  $-D_e$  of -2.1 kcal/mol, in good agreement with our MM result for the T-shaped dimer. In the case of the toluene dimer, Neusser and Krause found a binding energy (*i.e.*  $-D_0$ ) of -3.46 kcal/mol, that they ascribe to not only dispersion, but also dipole-dipole interactions. This value is in excellent accord with our ab initio estimate of  $-D_e = -3.43$  kcal/mol for the sandwich structure. The prediction from molecular mechanics for this arrangement is, however, 0.8 kcal/mol too repulsive, although one should keep in mind that if the ZPE is included, this difference should be reduced. Our estimate for the ZPE term, computed for the T-shaped benzene dimer, at the MP2/6-31G\* level of approximation, is 0.62 kcal/mol. As noted by Hobza

*et al.*, this quantity is likely to be similar for the stacked, the T-shaped, and the parallel-displaced structures. We further contend that the ZPE for the toluene dimer should be close enough to that of the benzene dimer.

At this stage, we have demonstrated, using both high-quality QM and MM calculations, that the energetic hierarchies of the T-shaped and the stacked motifs of the benzene and the toluene dimers are at variance. We, however, passed over the parallel-displaced structures, since the purpose of this paper was not to investigate the complete conformational space of these dimers. Nevertheless, at least in the case of the gas-phase benzene dimer,<sup>27,28,60</sup> the parallel-displaced state has been shown to be a key feature of the potential energy surface. Recently, Jaffe and Smith estimated, at the MP2/6-311G(2d,2p) level, its BSSE-corrected binding energy ( $C_{2h}$  geometry) to be -3.33 kcal/mol—*i.e.* 0.49 kcal/mol lower than the T-shaped form. The equilibrium distance between the centers of mass of the two benzene rings was found at 3.7 Å. For this particular motif, our MM calculations led to a binding energy of -2.33 kcal/mol, which is 0.06 kcal/mol lower than the estimate for the T-shaped structure. It is worth pointing out that Hobza *et al.*<sup>27,28</sup> reported a difference in binding energies of 0.27 kcal/mol between the parallel-displaced and the T-shaped motifs. Whereas the Cornell *et al.* force field<sup>48</sup> appears to be successful in reproducing the hierarchy of the conformational energies characteristic of the benzene dimer, the predicted separation of 4.7 Å denotes a lack of van der Waals attraction between the two aromatic moieties—which, surprisingly, was not witnessed for the stacked and the T-shaped arrangements. Singularly, in the case of the toluene dimer, the minimum energy parallel-displaced anti-parallel structure corresponds to a separation of only 3.9 Å. This is likely to result from enhanced van der Waals interactions, due to the presence of the methyl groups. The binding energy of -2.83 kcal/mol is 0.22 kcal/mol lower than that of the stacked motif, which concurs with our preliminary QM results,<sup>62</sup> and further indicates that, for both the benzene and the toluene dimers, the parallel-displaced conformation is lower in energy than the T-shaped, as well as the stacked structures. Considering, however, the orientation-averaged free energy profiles in Figure 2, one may note that the separation of the aromatic rings at the minimum is representative of a T-shaped motif (a skewed perpendicular arrangement, in fact) rather than a sandwich one. This fact is undoubtedly rooted into the lower entropy associated to the parallel structures, in comparison with T-shaped or V-shaped dimers.

An interesting point, underlined by Hunter,<sup>36</sup> concerns the alleged poor description of electrostatic interactions by means atom-centered point charge models. It is true that, as has been shown extensively, quadrupole-quadrupole interactions are the predominant electrostatic interactions in the benzene dimer, and such contributions are not evaluated explicitly in “minimalist” potential energy functions, like the one employed herein. It should, nonetheless, be pointed out that these interactions are in fact taken into account *indirectly*, since, for the present  $\pi$ -systems, quadrupoles can be reproduced from simple monopoles with an acceptable accuracy. This is clearly illustrated in Table 4, where we have confronted the “reference” Buckingham traceless multipole moments—*i.e.* the expectation values  $\langle r_i^{(n)} \rangle$ —to those regenerated from the point charge models. As can be observed, the largest deviation between the RHF/6-31G\*\* quadrupolar moments and the regenerated ones never exceeds 0.5%. The accord even holds, in the case of toluene, for octupoles, and, to a lesser extent, for hexadecapoles. The

(60) Jaffe, R. L.; Smith, G. D. *J. Chem. Phys.* **1996**, *105*, 2780.

(61) Smith, G. D.; Jaffe, R. L. *J. Phys. Chem.* **1996**, *100*, 9624.

(62) Jaffe, R. L. Work in progress, 1996.

**Table 4.** Comparison between the “Reference” Hartree–Fock Cartesian Traceless Multipole Moments of Benzene and Toluene and Those Regenerated from Atom-Centered Potential Derived Charge Models, Using the Split-Valence 6-31G\*\* Basis Set

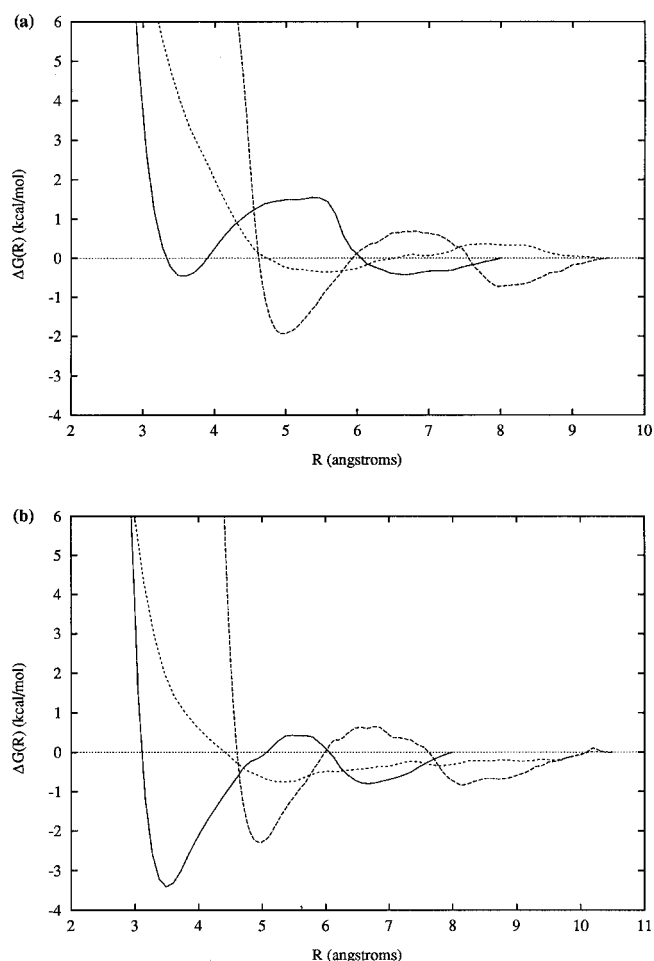
multipole moment <sup>a</sup>	benzene		toluene	
	potential derived charges	ab initio	potential derived charges	ab initio
$\mu_x$			-0.290	-0.291
$\mu_y$			-0.001	-0.004
$\mu_z$			-0.001	0.029
$\mu_{\text{total}}^b$			0.290	0.292
$\Theta_{xx}$	4.121	4.144	4.098	4.122
$\Theta_{yy}$	4.121	4.144	3.756	3.769
$\Theta_{zz}^c$	-8.243	-8.287	-7.854	-7.891
$\Omega_{xxx}$			8.304	8.306
$\Omega_{yyy}$			0.176	0.178
$\Omega_{zzz}$			1.397	1.313
$\Omega_{xyy}$			1.745	1.838
$\Omega_{zzz}$			-10.049	-10.144
$\Omega_{yyz}$			-1.531	-1.386
$\Phi_{xxxx}$	18.502	22.991	6.862	10.502
$\Phi_{yyyy}$	18.502	22.991	9.766	14.837
$\Phi_{zzzz}$	49.339	61.311	52.908	58.959
$\Phi_{xxyy}$	6.167	7.664	18.140	16.810
$\Phi_{xxzz}$	-24.670	-30.655	-25.002	-27.312
$\Phi_{yyzz}$	-24.670	-30.655	-27.906	-31.647

<sup>a</sup>  $\mu_\alpha$  in D,  $\Theta_{\alpha\beta}$  in D Å, and  $\Omega_{\alpha\beta\gamma}$  in D Å<sup>2</sup>. <sup>b</sup> Toluene experimental dipole moment:  $\mu_{\text{exp}} = 0.36$  D. <sup>c</sup> Benzene experimental quadrupole moment:<sup>71</sup>  $\Theta_{zz/\text{exp}} = -8.7 \pm 0.5$  D Å.

general agreement between experimental, quantum mechanical, and molecular mechanical binding energies is also suggestive that models limited to potential derived net atomic charges can be sufficient to ensure a correct reproduction of higher order multipole moments. At the present time, however, it is not clear whether the nice performance of electrostatic potential derived charges for the specific examples reported here will hold for more complex  $\pi$ -systems. Lastly, the good behavior of our molecular mechanical calculations indicates that the van der Waals and electrostatic contributions of the macromolecular force field are appropriately balanced, which, in our opinion, is a *sine qua non* condition for a correct description of  $\pi$ - $\pi$  interactions.

**$\pi$ - $\pi$  Interactions in an Aqueous Solution.** The PMFs depicted in Figure 3 characterize the free energy changes for bringing two benzene, or two toluene, molecules toward each other, in TIP3P water. As may be seen on this set of graphs, the trend for orientational preference witnessed in the gas phase appears to hold in an aqueous solution. In particular, hydrophobic effects, which are anticipated to favor compact sandwich arrangements, lead, in the case of the stacked toluene dimer, to a contact minimum of  $-3.41$  kcal/mol occurring at  $3.5$  Å. This is approximately  $0.9$  kcal/mol lower than the corresponding gas-phase minimum. In addition, the environment is responsible for the emergence of a so-called “solvent-separated” minimum of  $-0.80$  kcal/mol located at  $6.7$  Å. Conversely, the contact minimum of the T-shaped toluene dimer, occurring at  $5.0$  Å, with a depth of  $-2.29$  kcal/mol seems to remain unaffected by the surroundings. Solvent effects, however, cause the appearance of a secondary minimum around  $8.1$  Å, with a free energy of  $-0.85$  kcal/mol.

Similarly, in the case of the benzene dimer, the aqueous environment is responsible for the presence of solvent-separated complexes, but hydrophobic effects, which should favor  $\pi$ -overlaps, are insufficient to lower the free energy of the sandwich structure below that of the point-to-face motif. The stacked benzene dimer possesses a contact and a solvent-separated minimum occurring respectively at  $3.6$  and  $6.7$  Å, with a free

**Figure 3.** Free energy profiles of the stacked (solid line), the T-shaped (long-dashed line), and the unconstrained (short-dashed line) benzene (a) and toluene (b) dimers, in TIP3P water.

energy of  $-0.47$  and  $-0.43$  kcal/mol. The T-shaped dimer is also characterized by a contact and a solvent-separated minimum, located at  $4.9$  and  $8.0$  Å, respectively, with the corresponding free energies of  $-1.94$  and  $-0.74$  kcal/mol. We find that these results agree very nicely with the findings of Linse<sup>29</sup> on a similar system: *ca.*  $-0.1$  and  $-0.74$  kcal/mol for the contact and the solvent-separated minima of the stacked benzene dimer, and  $-1.9$  and  $-0.4$  kcal/mol for the T-shaped dimer.

Interestingly enough, the PMFs representative of the unconstrained benzene and toluene dimers tend to indicate that, for both solvated systems, the orientational preference corresponds to neither a sandwich structure nor a T-shaped one—albeit their unique minima, located at  $5.6$  and  $5.4$  Å, respectively, are suggestive of a favored skewed perpendicular arrangement. The computed average angles,  $\langle\varphi\rangle$ , formed by the normals  $\mathbf{n}_1$  and  $\mathbf{n}_2$  of the aromatic moieties, at the intermolecular separation characterizing the unconstrained minima (see Table 2), over 50 ps of MD trajectory, are  $94^\circ$  for the benzene dimer and  $124^\circ$  for the toluene dimer, with a clear preferential sampling toward a T-shaped-like form. As commented on by Linse,<sup>31</sup> we observed from the  $(\mathbf{n}_1, \mathbf{D}_1\mathbf{D}_2)$  versus  $(\mathbf{n}_2, \mathbf{D}_1\mathbf{D}_2)$  distribution (see Figure 1) that the presence of V-shaped motifs—*viz.* ( $62^\circ, 127^\circ$ ) and ( $43^\circ, 122^\circ$ ), for the benzene and the toluene dimers, respectively—is far from negligible. It is also worth pointing out that the associated free energies are much smaller than those characterizing the constrained point-to-face and face-to-face dimers, as a result of significant entropic effects. Jorgensen and Severance<sup>30</sup> found a much stronger attraction of the benzene dimer in water (*viz.*  $-1.5$  kcal/mol near  $5.5$  Å). In contrast,

the estimate of Linse<sup>31</sup> of about  $-0.5$  kcal/mol, for the same system, is in much better accord with our free energy difference of  $-0.36$  kcal/mol. Finally, we should underline that, regardless of the force field employed, parallel-displaced structures, which correspond to an intersolute separation slightly smaller than for true sandwich motifs, are not observed. This could be ascribed, in part, to hydrophobic effects, since parallel-displaced dimers expose a remarkably larger area toward the solvent than stacked dimers.

Direct comparison of the above results with experiment is feasible by evaluating the association constant,  $K_a$ , for each energy profile.<sup>63</sup> This quantity may be obtained for a dilute solution by integrating the free energy profile to an appropriate separation,  $R_{\text{cut}}$ , which delineates the limit of association:

$$K_a = 4\pi \int_0^{R_{\text{cut}}} r^2 e^{-\Delta G(r)/RT} dr \quad (1)$$

Another possible source of comparison between theoretical and experimental data requires the estimation of the second virial coefficient  $\bar{B}$ , from the McMillan–Mayer theory:<sup>64</sup>

$$\bar{B} = 2\pi \int_0^\infty r^2 [1 - e^{-\Delta G(r)/RT}] dr \quad (2)$$

The calculated association constants for the stacked, the T-shaped, and the orientationally averaged benzene dimers<sup>65,66</sup> are 0.16, 3.07 and 0.80  $\text{M}^{-1}$ , respectively ( $R_{\text{cut}}$  was chosen arbitrarily to be the intersolute distance at which  $\Delta G(r) = \text{max}$ , hence limiting the integration over the region of contact association). The latter is in excellent agreement with the experimental value of 0.85  $\text{M}^{-1}$ , provided by Tucker and Christian.<sup>67</sup> However, the accord between the theoretical and experimental osmotic second virial coefficients is less satisfactory. Whereas Tucker and Christian, and Rossky and Friedman<sup>68</sup> respectively reported experimental values of  $-1177$  and  $-1001 \text{ \AA}^3 < \bar{B} < -276 \text{ \AA}^3$ , the computed quantities for the face-to-face, point-to-face, and unconstrained arrangements are  $-89$ ,  $-2834$ , and  $+248 \text{ \AA}^3$ . For an orientationally averaged benzene dimer, Jorgensen and Severance found an association constant and an osmotic second virial coefficient of 2  $\text{M}^{-1}$  and  $-6700 \text{ \AA}^3$ , respectively, hence overestimating the association. On the other hand, Linse, for a similar system, slightly underestimated it, with  $K_a = 0.7 \text{ M}^{-1}$  and  $\bar{B} = -1200 \text{ \AA}^3$ .

Molecular association is substantially stronger in the case of the toluene dimer. The calculated association constants for the stacked, the T-shaped, and the unconstrained arrangements are 14.8, 4.77, and 4.39  $\text{M}^{-1}$ , respectively. Just like for the T-shaped benzene dimer, it is likely that the association constant characterizing the stacked toluene dimer is overestimated. The osmotic second virial coefficients are  $-12794$ ,  $-5005$ , and  $-1360 \text{ \AA}^3$ , for the face-to-face, point-to-face, and unconstrained complexes, respectively. It would seem that measured deviations from Henry's law for this particular system are not available in the literature, thus precluding a direct comparison of our data with experiment. Although benzene and toluene have similar solubilities in water (*viz.*  $-0.77$  and  $-0.88$  kcal/mol, respectively<sup>53</sup>), the lower vapor pressure of toluene makes

studies of the equilibrium distribution of the latter between vapor and aqueous solution phases particularly difficult.

**Analysis of Phe–Phe Interactions in Proteins.** The various molecular and quantum mechanical computations reported herein have demonstrated that the orientational preferences for the benzene and the toluene dimers are clearly different—both in a *vacuum* and in an aqueous solution. It is then legitimate to wonder whether or not the benzene dimer constitutes the best prototypical system to rationalize the trends in  $\pi$ - $\pi$  interactions observed in protein crystallographic structures, especially if one admits that toluene models the Phe side chain somewhat more accurately than benzene. On the basis of their exhaustive analysis of protein structures, Hunter *et al.*<sup>8</sup> underlined that sandwich arrangements of the Phe aromatic rings are seldom encountered, because, just like for the benzene dimer, repulsive electrostatic quadrupole–quadrupole forces dominate long-range attractive dispersion interactions. Yet, our results on the toluene dimer suggest that the rarity of stacked Phe motifs should be explained by other factors. In particular, the most favorable arrangement of the Phe side chains should, in principle, be a parallel one, for which not only the aromatic rings, but also the methylene groups are stacked, hence leading to an enhanced dispersion contribution. However, in the light of our Protein Data Bank<sup>69</sup> (PDB) analysis,<sup>70</sup> carried out over 404 nonredundant structures, it would seem that such true sandwich structures are scarce because of sterical reasons. In addition, the low entropy stacked arrangement of the Phe side chains offers less possibility for secondary interactions with the surroundings than the T-shaped motif—for example, interactions with cationic (Lys) or hydroxyl (Ser, Thr) functional groups, or even water. As illustrated in Figure 4, such ancillary interactions are, indeed, mainly found with T-shape arrangements of the Phe rings, which expose three aromatic faces to their immediate environment. Similarly, it is observed that, as expected, parallel-displaced motifs offer more opportunities for secondary interactions than sandwich structures.

Our results concur with the study of Serrano *et al.*<sup>9</sup> on aromatic–aromatic interactions as a stabilizing factor in proteins. First, they estimate that direct  $\pi$ - $\pi$  interactions between aromatic pairs contribute to  $-1.3$  kcal/mol, which is not out-of-line with our estimates in the gas phase. Second, these authors underline the critical role of additional interactions between the aromatic rings and neighboring functional groups on the overall stability of the protein. For instance, Matouschek *et al.*<sup>74</sup> have estimated that, in barnase, the interaction between the methylene group of Thr<sup>16</sup> and the aromatic face of Tyr<sup>17</sup> contributes for  $-1.9$  kcal/mol. Considering the magnitude of this interaction, it is not surprising that pairs of aromatic side chains will preferentially orient themselves exposing three faces (*i.e.* perpendicular-type arrangement) to the surroundings, rather than two (*i.e.* sandwich-type arrangement).

## Conclusions

In this study, we have endeavored to investigate the key differences in the orientational preference of the benzene and

(69) Abola, E. E.; Bernstein, F. C.; Bryant, S. H.; Koetzle, T. F.; Weng, J. In *Crystallographic Databases—Information Content, Software Systems, Scientific Application*; Allen, F., Sievers, R., Eds.; Data Commission of the International Union of Crystallography: Bonn/Cambridge/Chester, 1978; p 107.

(70) Maigret, B.; Chipot, C. Unpublished results, 1996.

(71) Battaglia, M. R.; Buckingham, A. D.; Williams, J. H. *Chem. Phys. Lett.* **1981**, *78*, 421.

(72) Lindley, P. F.; Bajaj, M.; Evans, R. W. *Acta Crystallogr., Sect. D, Biological* **1993**, *49*, 292.

(73) Holmes, M. A.; Stenkamp, R. E. *J. Mol. Biol.* **1991**, *220*, 723.

(74) Matouschek, A.; Kellis, J.; Serrano, L.; Fersht, A. R. *Nature* **1989**, *340*, 122.

(63) Shoup, D.; Szabo, A. *Biophys. J.* **1982**, *40*, 33.

(64) McMillan, W.; Mayer, J. J. *Chem. Phys.* **1945**, *13*, 276.

(65) Friedman, H. L.; Krishnan, C. V. *J. Solution Chem.* **1973**, *2*, 119.

(66) In the definition of both  $K_a$  and  $\bar{B}$ ,  $\Delta G(r)$  represents an effective—*i.e.* solvent-averaged and orientation-averaged—potential of mean force between the two aromatic moieties, at a separation “ $r$ ”. Estimates of these quantities for the constrained geometries have clearly a different reference, and are, as a result, not directly comparable.

(67) Tucker, E. E.; Christian, S. D. *J. Phys. Chem.* **1979**, *83*, 246.

(68) Rossky, P. J.; Friedman, H. L. *J. Phys. Chem.* **1980**, *84*, 587.

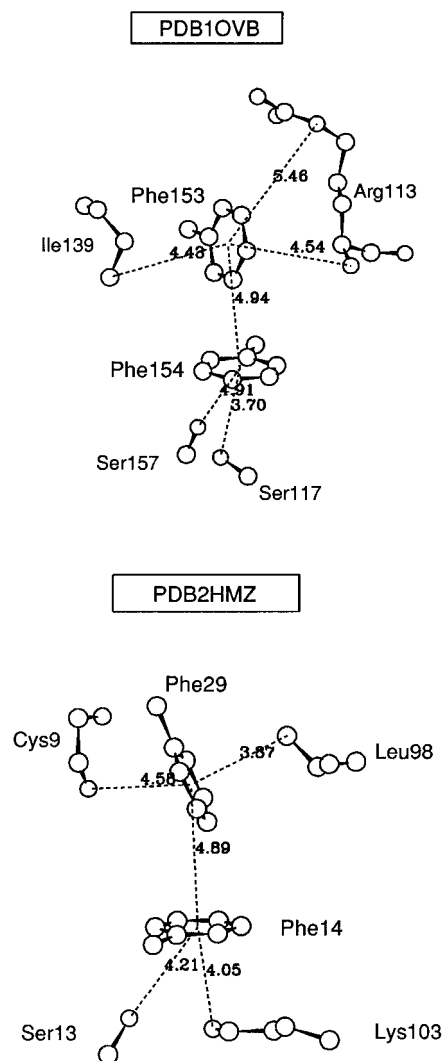


**Figure 4.** Examples of secondary interactions associated to  $\pi$ - $\pi$  phenylalanine-phenylalanine interactions in the iron transport protein ovotransferrin<sup>72</sup> (1OVb) and in the oxygen transport protein hemerythrin<sup>73</sup> (2HMZ). All distances in Å.

the toluene dimers. Whereas the first system has been hitherto employed extensively as a paradigm for rationalizing  $\pi$ - $\pi$  interactions in protein crystallographic structures, why not the second? Especially if one considers that toluene constitutes a better model of the Phe side chain than the simpler benzene. Thorough analysis of the PDB has revealed that sandwich

arrangements, unlike perpendicular ones, of the Phe residues are not common in proteins, which agrees with the calculated 0.78 kcal/mol free energy difference between the stacked and the T-shaped motifs of the prototypical benzene dimer. Our estimates of the association free energies of the face-to-face and point-to-face dimers of toluene, in the gas phase, as well as in an aqueous solution, reflect, however, an opposite tendency. The attractive dispersion term, reinforced by the presence of the methyl group, counterbalances the unfavorable electrostatic quadrupole-quadrupole repulsion, thus causing the sandwich structure of the toluene dimer to become energetically more favorable than the T-shaped motif.

The conflict between the orientational preferences of the benzene and the toluene dimers suggests that Phe side chains in proteins cannot be modeled by simple benzene rings to understand why perpendicular arrangements are more frequently encountered than sandwich ones. This assertion does not imply that toluene necessarily constitutes a more appropriate model to rationalize orientational trends in  $\pi$ - $\pi$  interactions in proteins. We believe, in fact, that in order to rationalize such trends, one should consider, in addition to the electrostatic and dispersion interactions between the aromatic moieties, possible sterical hindrances and ancillary interactions between the aromatic rings of Phe pairs and appropriate neighboring functional groups.

An interesting issue that should be underlined here is the generally good agreement between our molecular mechanical and high-quality quantum mechanical calculations and experiment. In particular, the binding energies reported in the present study compare well with the experimental ones obtained by Neusser and Krause from breakdown measurements.<sup>37</sup> Although "minimalist" potential energy functions, like the one employed in this work, often limit their electrostatic description to atom-centered point charges, reproduction of higher-order moments, such as quadrupoles, for both benzene and toluene is adequate. Interactions between these multipole moments are included implicitly in molecular mechanical calculations, and their balance with the van der Waals contribution is the key for a proper representation of  $\pi$ - $\pi$  interactions.

**Acknowledgment.** The authors wish to thank Drs. C. Millot and J. G. Ángyán for many stimulating discussions. C.C. is indebted to the Roussel Uclaf Company (France) for his doctoral fellowship and P.A.K. is grateful to N.S.F.-CHE-94-17458 and N.I.H.-GM-29072 for research support. R.L.J. acknowledges computer time from the San Diego Super Computer center.

JA961379L